April 5, 2006

Ken Zweibel
National Renewable Energy Laboratory
1617 Cole Boulevard
Golden, CO 80401

Re: NREL Subcontract #ADJ-1-30630-12

Dear Ken,

This report covers research conducted at the Institute of Energy Conversion (IEC) for the period from January 10, 2006 to February 15, 2006, under the subject subcontract. The report highlights progress and results obtained under Task 1 (CdTe-based solar cells).

Task 1 – CdTe-based solar cells

Summary: The CdTe cell fabrication effort focused on CdTe deposition and post deposition processing to increase throughput and raise baseline cell efficiency. The effect of carrier gas composition and substrate temperature on vapor transport (VT) CdTe film growth and device performance was evaluated. Vapor $CdCl_2$ treatments, which allow the treatment temperature to be separated from the $CdCl_2$ and O_2 concentration, were refined to allow a new baseline process to be defined with treatments ~ 2 minute in duration. Reduction in treatment time required increasing the treatment temperature of the CdTe/CdS and maintaining the partial pressures of $CdCl_2$ and O_2 to ~5 mTorr and 120 Torr, respectively. Similarly, the aniline photo-activated surface treatment was refined to permit effective Te formation in less than 5 minutes, by increasing the intensity of the incident light. In the area of device performance, analysis of J(V) curves has indicated that most CdTe cells can be described with three circuit elements: by a single forward diode (given by A, J_o), a resistance (R), and a voltage dependent photocurrent ($J_{L0} * \eta(V)$). Systematically determining these parameters and evaluating their impact on efficiency shows that our typical VT device with 12% efficiency could be 14% efficient in the absence of R and voltage dependent collection. This sets an upper limit based on the junction recombination.

VT Deposition

The VT system was designed for He carrier gas. From a design perspective, He was chosen for its high diffusivity and thermal conductivity. From a manufacturing perspective, other gases, such as N_2, warrant investigation. The effect of other carrier

gases was thus investigated with respect to growth rate, utilization, film morphology, and device performance. In the VT chamber, we distinguish between the carrier gas, which passes through the source ampoule and becomes saturated with Cd and Te_2 vapor, and the "background" gas, into which the vapor enters and through which the substrate passes during film growth. Depositions were carried out with He, N_2 and Ar as carrier and background gases at 20 Torr using a source temperature T_{sou} = 850ºC, substrate temperature T_{sub} = 550ºC, and translation speed = 1.25 cm/min. Substrates were CdS (60 nm) /Ga_2O_3/SnO_2 (TEC-15). The carrier gas was admitted at 20 sccm and the background gas contained a partial pressure of O_2 = 100 mTorr. Table I shows the resulting film thickness, CdTe utilization (mass gained on 10 x 10 substrate/mass lost from the source), grain size and roughness, expressed as the root-mean square (rms) deviation from the average thickness.

Table I. VT CdTe film properties obtained with different carrier gases.

Deposition	Carrier/ Background Gas	Film Thk (μm)	CdTe Util (%)	Mean GS (μm)	Film rms (nm)
185	He/He	6.6	51	9	351
191	He/He	5.0	40	9	224
186	N_2/He	6.8	47	9	408
188	Ar/He	7.8	45	13	164
190	N_2/N_2	5.3	51	9	236
189	Ar/Ar	11.5	44	18	171

Overall, similar results were obtained for He and N_2 gas combinations but thicker films and larger grain size were obtained for depositions containing Ar, suggesting a dramatic alteration of the heat transfer within the source manifold. The utilization was independent of carrier gas and resulting film thickness, while the film thickness and grain size increased for Ar gas. The roughness data, determined by atomic force microscopy (AFM), suggests that the Ar-deposited films were smoother; however, the large grain size restricted AFM area sampling (20 x 20 μm), so the low values obtained for the large-grained Ar samples are not representative of the total area roughness. Contact profilometry with a Dektak system indicated a peak-to-valley roughness of ~300 nm on the samples deposited with Ar carrier gas. Note that all VT films exhibit random crystallographic orientation with respect to the substrate, unlike PVD films which preferentially nucleate along the <111> axis.

Solar cells were fabricated using vapor $CdCl_2$ treatment for 2 minutes, with the sample at 480ºC, in an atmosphere containing 3 mTorr $CdCl_2$ and 120 Torr O_2. Back contact was made using aniline etch followed by electron beam evaporation of eight 0.36 cm^2 Cu/Ni contacts per sample. The average device performance and best cell performance are listed in Tables II and III, respectively. Note that the series began and ended with runs using He/He which was our standard process. They both had similarly poor performance, validating the good results with Ar and N_2 and verifying that they are not due to drift of some other random process variable.

Table II. ***Average*** cell performance (8 cells per sample) for CdTe deposited in different carrier gases.

Piece	Carrier/Background Gas	Thk (μm)	V_{oc} (mV)	J_{sc} mA/cm^2	FF (%)	η (%)
185.1	He/He	6.6	581	25.2	50.6	7.4
186.1	N_2/He	6.8	749	24.2	56.9	10.3
188.1	Ar/He	7.8	637	23.6	51.9	8.5
189.2	Ar/Ar	11.5	799	23.7	63.8	12.1
190.1	N_2/N_2	5.3	785	23.7	65.3	12.1
191.1	He/He	5.0	661	22.3	48.8	7.2

Table III. ***Best*** cell performance for samples of Table II with CdTe deposited in different carrier gases.

Piece	Carrier/Background Gas	Thk (μm)	V_{oc} (mV)	J_{sc} (mA/cm^2)	FF (%)	η (%)	QE @ 400 nm
185.1	He/He	6.6	635	25.9	55.3	8.9	0.68
186.1	N_2/He	6.8	787	24.2	60.7	11.5	0.52
188.1	Ar/He	7.8	778	23.8	66.5	12.3	0.40
189.2	Ar/Ar	11.5	804	23.8	66.4	12.7	0.44
190.1	N_2/N_2	5.3	796	24.3	69.4	13.4	0.42
191.1	He/He	5.0	693	23.0	52.6	8.4	0.39

The highest average and best cell performance was obtained for depositions with Ar/Ar and N_2/N_2 carrier gas/background gas combinations. The averages of 8 cells were also quite high (12%), indicating good uniformity as well as efficiency. Surprisingly, the samples deposited in He gave comparatively poor performance; in the case of run 185, the QE at 400 nm is very high, suggesting that the CdS film for this run was thinner than expected, resulting in low V_{oc} and FF.

Efforts to enhance V_{oc} in VT devices are presently focused on controlling the as-deposited CdTe properties by altering the conditions during film growth. In VT, the important control parameters that can be easily separated are CdTe purity, source temperature, substrate temperature, translation speed and ambient composition. The data above shows that the carrier and background gases affect the device quality, and we accordingly changed the baseline condition to N_2. The on-going effort is fabrication of devices with CdTe deposited using N_2 carrier gas vapor at higher temperatures, i.e. up to 600ºC, and at reduced growth rate compared to the baseline devices.

Vapor $CdCl_2$ Processing

The $CdCl_2$ treatment promotes interdiffusion of CdS and CdTe films due to the thermodynamic driving force for alloy formation. Since CdTe is typically >20x thicker than CdS and since the CdS solubility in CdTe is 2x that of CdTe in CdS, the CdTe film acts as sink for CdS, resulting in the eventual consumption of the CdS film. The

diffusion process is enhanced along grain boundaries and by the presence of $CdCl_2$ and O_2 in the ambient. Our previous standard was 420°C for 20 min. Recent experience has shown that to first-order, cell performance can be maintained with shorter treatments by increasing the treatment temperature. Vapor treatment allows this to be carried out a controllable $CdCl_2$ concentration, since the $CdCl_2$ source is thermally isolated from the CdTe sample. 2D modeling of the interdiffusion in VT films with 5 μm wide grains suggests that for treatment in 9 mTorr $CdCl_2$ and 100 Torr O_2, nominally similar CdS consumption is obtained for temperature/time treatments of 420ºC/20 min, 480ºC/2 min, and 495ºC/1 min. The graphical output of the 2D model of S concentration versus depth is shown in Figure 1 and was run for 5 micron thick films with 5 micron wide grains using diffusion coefficients previously determined for different T, $p(O_2)$ and $p(CdCl_2)$. Integration of the curves with the solubility limits at the given temperatures allows the equivalent CdS film thickness to be predicted.

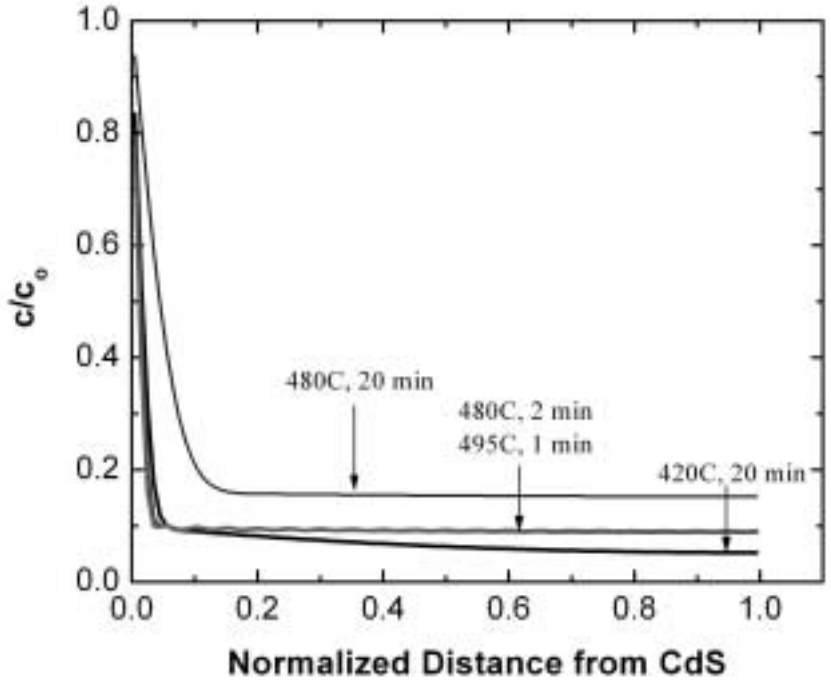

Figure 1. Calculated S concentration (c/c_o) versus normalized distance from CdS-CdTe interface. Note that 480°C for 2 min and 495°C for 1 min yielded essentially identical profiles.

In the figure, the bulk and grain boundary contributions are apparent by the steep and flat regions, respectively. For the typical baseline treatment, at 420ºC for 20 minutes, the least alloy formation is obtained, with an equivalent CdS film thickness consumed of only 20 nm. This corresponds extremely well with the measured final CdS thickness after cell fabrication and removal of the CdTeS absorber layer (selective citric acid etch). For the shorter cases, at 480ºC for 2 minutes and 495ºC for 1 minute, the equivalent CdS thicknesses consumed are higher = 40 nm. An extreme case, at 480ºC for 20 minutes, shows consumption of 100 nm of CdS, which would eliminate the CdS layer in these VT devices.

Table IV shows cell performance for CdTe cells fabricated with vapor $CdCl_2$ treatment at 480ºC with $CdCl_2$ time from 1 to 4 minutes. The CdTe samples were from a single deposition using N_2 carrier gas. The QE at 400 nm provides a quantitative measure of the final CdS film thickness. In the table, the final CdS film thickness decreases progressively with increasing treatment time over the treatment time range. Given that the starting CdS thickness was 90 nm, the quantity of CdS consumed is similar to that predicted by the diffusion model above. In this sampling, the decrease in CdS thickness has no systematic effect on V_{oc}; in fact, the lowest V_{oc} was obtained for the shortest treatment time, not the longest, indicating that the overall cell fabrication process is tolerant to and allows controllable CdS consumption.

Table IV. Best cell performance for CdTe deposited using N_2 carrier gas and vapor $CdCl_2$ treatment at 480ºC with different $CdCl_2$ time.

Piece	$CdCl_2$ HT (min)	V_{oc} (mV)	J_{sc} (mA/cm^2)	FF (%)	η (%)	QE @ 400 nm (%)	Final dCdS (nm)
190.2	1	783	23.6	66.6	12.3	40	60
190.1	2	796	24.3	69.4	13.4	42	58
190.4	2	813	23.6	66.2	12.7	44	55
190.6	2.5	800	23.3	65.1	12.2	44	55
190.3	4	819	24.3	64.6	12.9	50	35

Aniline Surface Treatment

The investigation of aniline etching of CdTe has continued along two paths: 1) understanding the chemistry and photo-activation and 2) adapting the etch for high processing throughput. We have previously reported aniline etching of CdTe under illumination produces a Te-rich surface layer that either form or occur via two mechanisms; photo-catalytic degradation of aniline at the CdTe surface and/or etching of CdTe by the NaCl and acid present in the etching bath in warm solutions. The former mechanism only occurs under illumination, while the latter only occurs at raised temperatures, ca. >40°C. To identify the optimum conditions for aniline etching for CdTe device processing, we fabricated a series of CdTe devices receiving various aniline etch treatments. Standard etching baths containing 0.1 M aniline, 0.001 M *p*-toluenesulfonic acid and 1 M NaCl were used to etch ~5 μm thick VT deposited CdTe/CdS substrates that had received solution $CdCl_2$ treatments.

The etch treatments carried out were: with and without aniline in solution under illumination without cooling, i.e. warmed by the illuminating lamp to ~45°C, and with and without aniline under illumination cooled in a jacketed beaker to ~20°C. Pieces were etched for 60 min with illumination on the glass side of the samples, before being removed from solution, rinsed with H_2O and contacted with saturated CuI/methanol spray and graphite paste, followed by a 20 min anneal at 190°C in Ar(g). The performance of the completed devices was poor with η = 6-8%, V_{oc} = 650 – 790 mV and FF = 40-55%.

This may be due to insufficient $CdCl_2$ treatment or back contact processing; however, some patterns in device performance with the different etch treatments are discernable. The lowest performance device had received the 'cooled aniline-free' treatment. These conditions are expected to produce the least surface Te and this is reflected in the device result. The best performing device was processed with the 'cooled with aniline' solution, suggesting that this condition produces the closest to optimum surface for back contact processing. The pieces etched in the un-cooled solutions, both with and without aniline, gave poorer results. This may suggest that the warm acid + salt mechanism may over-etch the surface and/or grain boundaries, leading to inferior contacts and device performance.

Since the rate of aniline reaction varies with illumination, a path to adapting the etch for high throughput processing is increasing the illumination and quantifying its effect on Te production and device operation. The experimental apparatus consists of an illumination source, a filter holder, a reaction vessel, a sample holder, and a cooling fan (Fig. 2). GIXRD using Cukα radiation at $\Omega = 0.5$ degree incident beam angle was used to determine relative quantities of Te and Te particle domain size formed on the CdTe surface. Extremely slow scans were taken to ensure acquisition of sufficient Te signal above background.

Figure 2. Apparatus used to investigate illumination effect on aniline reaction. The power to the ELH bulb is controlled by a variac. The sample is immersed in the solution shown to the right.

Table V lists various aniline etch conditions, resulting Te peak intensity and area, and device performance for cells made with CdTe deposited in a single deposition in He ambient and treated in $CdCl_2$:O_2 vapor at 480ºC for 2 minutes. To minimize heating of the solution, an infrared-absorbing glass filter was placed in front of the reaction vessel. The bath temperature reached 35ºC after 5 minutes of treatment with the ELH lamp at

100V at a distance of 15 cm. In the table, the total incident flux was measured using an Eppley radiometer located at the sample position.

Table V. Aniline reaction conditions, GIXRD results (particle size and peak area) and best cell performance for 2 cm^2 area VT CdTe samples. All samples were illuminated directly on the CdTe surface except 173.4c. In column 2, BP = band pass and CO= cutoff. All samples except 173.3a, 6a and 6c were treated for 10 minutes. Flat means sample was not immersed but held horizontal and coated with aniline.

Piece	Aniline Illumination Condition	Flux (mW/cm^2)	GIXRD Te(110) Part Size (nm)	GIXRD Te(110) Peak Area (Counts)	V_{oc} (mV)	J_{sc} (mA/cm^2)	FF (%)	η (%)	QE @ 400 nm
173.3a	None	0	0	0	n/a	n/a	n/a	n/a	n/a
173.6a	None	0	0	0	792	21.6	64.3	11.0	
173.6b	Dark, 10 min	0	26	92	778	20.8	61.0	9.9	
173.6c	Dark, 30 min	0	42	108	767	21.0	69.2	11.2	
173.5c	Hg Vapor Lamp	11	80	70	779	22.0	56.2	9.6	
173.3a	ELH, both sides	25	8	1098	798	21.7	59.6	10.3	
173.3b	ELH, 550 nm BP	25	12	184	799	21.7	53.9	9.3	0.32
173.3c	ELH, RG780 CO	25	6	252	787	21.9	57.1	9.9	
173.4a	ELH, both sides	165	9	564	789	22.0	61.6	10.7	
173.4b	ELH, CdS dark	165	10	244	798	22.5	60.5	10.9	
173.4c	ELH, Thru CdS	165	12	104	792	21.9	59.6	10.3	
173.5a	ELH, Flat	165	5	544	755	19.5	49.5	7.3	
173.5b	ELH, Flat,Shield	165	9	280	804	21.9	58.4	10.3	

Samples with no etch showed only CdTe reflections in the GIXRD patterns. Reacting in dark or light produced the Te (101) reflection. For reaction in the dark for 10 and 30 minutes, similarly thin Te deposits resulted; from prior calibrations of Te (101) to CdTe (111) peak area ratios, the Te film average thickness is estimated to be <1 nm. Illumination with Hg vapor lamp at 11 mW/cm^2 produced similar Te thickness as the dark etched samples but the largest particle size in the entire group, i.e., the sharpest Te diffraction line profile. The thickest Te layers were produced by treatments with unfiltered ELH at 25 mW/cm^2 with illumination on both sides (173.3a). Higher intensity produced Te layers with intermediate thickness, suggesting a steady state reaction in which excess Te is dissolved from the surface. For reaction performed with illumination through the CdS only (173.4c), the quantity of Te formed is about half of that formed with illumination only on the CdTe (173.4b). The solution volume has little effect on the quantity of Te obtained, as shown by the samples held flat and coated with 0.1 cc of aniline solution (173.5a and 5b). In the case of 5a, light was allowed to reach the sample from all sides, while in case 5b, only light incident on CdTe was allowed. The relatively low Te deposits obtained for illumination with the Hg lamp, the 550 nm band pass filter, and through only the CdS does seems to suggest that total intensity reaching the specimen is the single most important factor affecting the quantity of Te formed in the 10 minute time span. Subsequent work with treatment times less than 10 minutes shows that equivalent Te quantity is formed at 100mW/cm^2 illumination for 4 minutes and, as above, drops off for longer times due to dissolving of Te. In the next report, XPS analysis will

be presented, showing that the new $CdCl_2$ vapor and aniline treatments only chemically alter the terminating 100 nm of the VT CdTe.

High Throughput Processing

The encouraging results obtained for reduced time of the $CdCl_2$ and aniline treatments presented above provided the basis for establishing a new baseline for high throughput post-deposition processing of VT CdTe solar cells. Tables VI and VII below show the average and best cell performance for samples processed from a single VT deposition carried out in He carrier gas. The average and best cell efficiency differ by 1% absolute. Although optimization of V_{oc} and FF are still required, the results suggest a wide processing latitude for choice of $CdCl_2$ treatment temperature (from 480ºC to 495ºC) and aniline treatment conditions. A notable result is cell efficiency >10% for 0.5 minute $CdCl_2$ treatment and 0.5 minute aniline treatment (198.5). In general, the aniline etch yields higher performance than the formerly employed BDH etch which penetrates the CdTe. The QE at 400 nm is very similar for all the cells in this set, as predicted by the 2D diffusion model results presented above, and shows that good processing consistency can be expected by these techniques. Thus, a viable post-deposition approach for fabricating cells with very thin CdTe absorbers has been achieved.

Table VI. Average cell performance (8 cells per sample) for 6 μm thick VT CdTe deposited at 11 μm/min on 60 nm $CdS/Ga_2O_3/SnO_2$ (TEC-15): Data ranked by increasing temperature of $CdCl_2$ vapor treatment.
Etch codes: BD2H = IEC baseline (Bromine/Dichrol/Hydrazine)
A/X/Y = Aniline/Lamp Power Setting (%)/Time (min)
Lamp power conversions (Eppley radiometer):
ELH @ 15 cm with Variac @ 60% = 130 mW/cm^2
ELH @ 15 cm with Variac @ 100% = 440 mW/cm^2

Piece	Trxn (C)	$TCdCl_2$ (C)	Time (min)	Etch	V_{oc} (mV)	J_{sc} (mA/cm^2)	FF (%)	η (%)
198.1	420	420	20	BD2H	736	23.5	57.8	10.0
198.4b	480	425	2	A/100/2	791	24.8	59.2	11.6
198.3a	480	425	2	A/60/5	802	24.8	60.7	12.1
198.4a	480	425	2	A/60/2	771	24.8	55.6	10.7
198.3b	480	425	2	A/60/1	779	25.3	55.5	10.9
198.5	490	425	0.5	A/60/0.5	740	24.9	51.3	9.5
198.2b	495	425	2	A/100/5	769	24.2	62.9	11.7
198.2a	495	425	2	A/60/5	744	23.7	58.8	10.4

Table VII. Best cell performance for samples of Table VI, with 6 μm thick VT CdTe deposited at 11 μm/min on 60 nm CdS/Ga_2O_3/SnO_2 (TEC-15): Data ranked by increasing temperature of $CdCl_2$ vapor treatment. Same codes as above.

Piece	Trxn (C)	$TCdCl_2$ (C)	Time (min)	Etch	V_{oc} (mV)	J_{sc} (mA/cm^2)	FF (%)	η (%)	QE @ 400 nm
198.1	420	420	20	BD2H	745	24.6	59.9	11.0	52%
198.4b	480	425	2	A/100/2	792	25.3	60.8	12.2	56
198.3a	480	425	2	A/60/5	804	24.7	63.3	12.6	52
198.4a	480	425	2	A/60/2	788	25.2	62.1	12.3	54
198.3b	480	425	2	A/60/1	783	25.7	58.0	11.7	55
198.5	490	425	0.5	A/60/0.5	775	25.0	52.5	10.2	58
198.2b	495	425	2	A/100/5	787	25.6	65.1	13.1	52
198.2a	495	425	2	A/60/5	775	24.0	66.7	12.4	52

Effect of Voltage Dependent Collection on FF and Efficiency

The JV data base from 2005 was analyzed to identify which of the 3 parameters – V_{oc}, J_{sc} or FF – was most directly influencing efficiency. There was poor correlation with V_{oc} or J_{sc} but good correlation with FF. Variability in FF has been a problem, with values typically <60% except for occasional pieces with FF~65-68%. Series resistance and shunting were not responsible for the variability, nor were they large enough to explain the consistently low values.

In the 2004 Annual Report, we presented an analysis of the voltage dependent photocurrent collection in CdTe solar cells, showing that the same analysis developed for a-Si solar cells could be applied to JV curves from devices from BP Solar, First Solar, U. Toledo and IEC to yield the voltage dependence collection efficiency η(V) from measurements at several intensities. It is well known that η(V) losses primarily influence the FF. We selected 3 recent devices having FF of 72, 62, 56% processed in the same week for comparison. JV parameters are given in Table VIII. Light and dark JV curves are in Figures 3a and 3b. They had minor differences in contact processing and $CdCl_2$ treatment but the variation in FF was greater than expected. JV was measured at 100, 10, 1% light and dark. The JV curve at 1% light was analyzed to determine A, J_o and R since analysis of the dark JV curves was not appropriate due to large light-dark crossover. Values are given in Table VIII. A, J_o are the same on all 3, consistent with same V_{oc}~0.79V, thus the junction quality or forward recombination current was not responsible for the different FF. Changes in FF were much greater than expected for R of a few Ohm-cms. So the JV curves at different intensity (J_1(V), J_2(V) etc) were analyzed to determine η(V'). Although the devices are not shunted (Fig. 3b), note that G_{sc}(=dJ/dV at 0V) in Table VIII increases monotonically with decreasing FF as expected for voltage dependent photocurrent collection.[1]

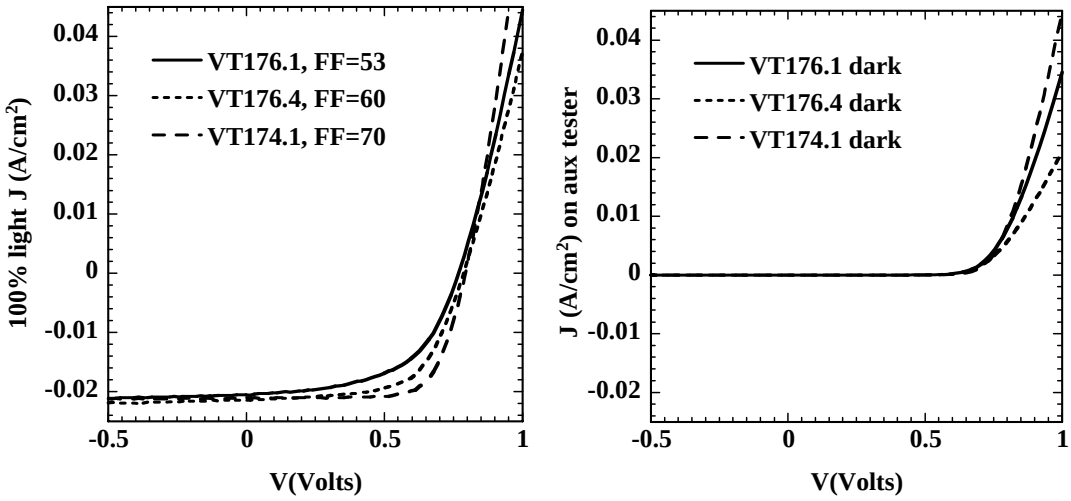

Figures 3a and 3b. Light and dark JV curves for three VT CdTe devices with differing FF.

The voltage dependent collection function η(V') was determined from difference of J(V') at 2 intensities

$$\eta_c(V') = [[J_1(V') - J_2(V')]/[J_{LO2} - J_{LO1}]] \qquad (1)$$

where V'=V-(J*R), as described elsewhere.[2] J_{L01} and J_{L01} are the maximum light current for each intensity 1; i.e. J at –0.5V where there are no recombination losses. Figure 4 shows η(V') obtained using the difference between 100 and 10% light for all three cells. Results were independent of which pair of light intensity was used. Clearly, the device with the highest FF has the least voltage dependent losses, i.e. the highest values of η(V'). Values of η(V') at V_{mp} decreased from 95 to 90 to 80% as the FF decreased from 72 to 62 to 56%.

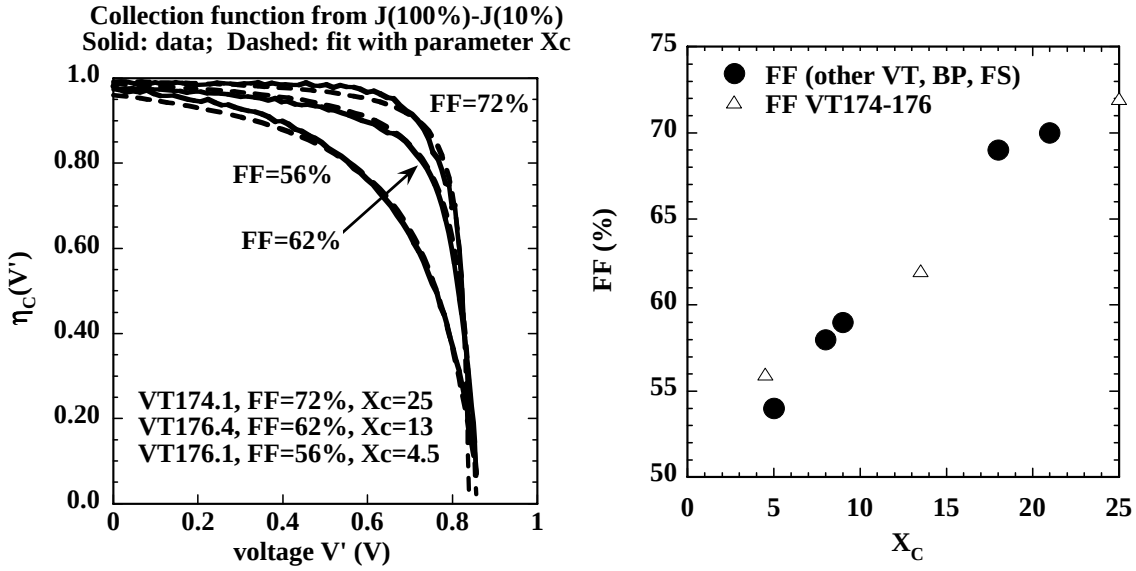

Figure 4 (left). η(V') for the three devices obtained from the difference of 100 and 10% light curves. The solid line is the data and dashed line is fit to equation 1 with X_c as the fitting parameter.

Figure 5 (right). Correlation between FF and X_c for 8 CdTe devices including the three analyzed here from VT174 or VT176.

The voltage dependent collection efficiency was also fit with model developed for a-Si p-i-n solar cells by Crandall as described elsewhere.[2] The model assumes the light is absorbed in a region of uniform field which decreases linearly with applied forward bias giving

$$\eta_c(V') = X(V')\left[1 - \exp\left(X(V')^{-1}\right)\right] \quad (2)$$

$$X(V') = X_C\left(1 - \frac{V'}{V_{FB}}\right) \quad (3)$$

where X_c is the primary fitting parameter representing minority carrier collection. V_{FB} is the flat band voltage which makes η(V')=0. The fit to the data is quite good as indicated in Figure 4 by the dashed lines. Best-fit values of X_c are given in Table VIII. Of the three primary causes for low FF - high forward recombination, R or η(V') – only η(V'), expressed through X_c, correlates with FF for these three cells. Further analysis on more samples would be needed to determine if lower X_c is due largely to lower electron mobility, lifetime or lower field.

Figure 5 shows data from 8 other CdTe devices, including those from BP Solar, First Solar and IEC. The FF is well correlated with X_c. Note that this trend is very similar quantitatively to results obtained from a large number of a-Si devices (see Fig. 14 of reference 2). This suggests that CdTe has the same voltage dependent collection mechanism as a-Si p-i-n cells.

Having established that voltage dependent collection is responsible for differences between these three cells, we can calculate their performance in the absence of $\eta(V')$ and R such that the FF would be determined only by forward diode recombination. Figures 6a and 6b show the power curve for the device with the lowest and highest FF for three cases: as measured, with effect of R removed, and with effects of R and $\eta(V')$ removed. Note that after correction for R and $\eta(V)$, the two devices, having 9.2 and 12.2% efficiency, are nearly the same, with 13.4 vs. 13.9%, respectively. This is to be expected since after correction R and $\eta(V)$, only junction losses due to the forward diode current remains to limit the FF, and these devices had nearly same A and Jo. Thus, our present processing has an upper limit of 14% determined by forward recombination current. Figure 6a also shows the power calculated from shifting the dark JV by J_{sc} after correcting for R. It is identical to the curve obtained from measured light JV with effects of R and $\eta(V')$ removed. This indicates superposition applies once these two losses are accounted for.

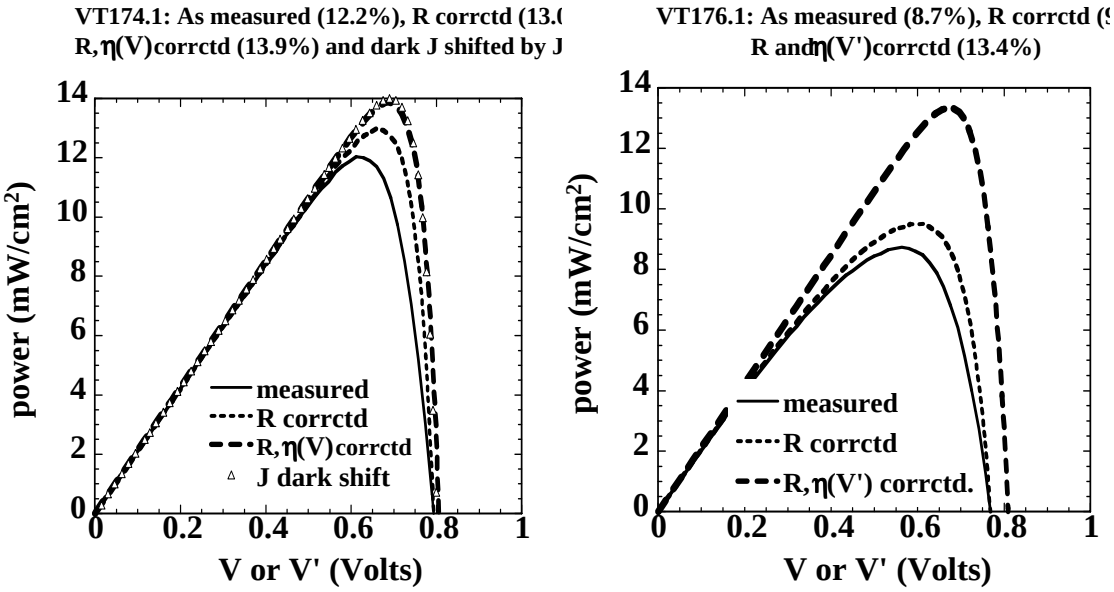

Figure 6a (left) and 6b (right). Power curves for VT174.1 and 176.1 as measured, after removing effect of R losses, and removing effect of R and $\eta(V')$. Fig. 6a also shows power for dark curve shifted by J_{sc} being identical to curve for R and $\eta(V')$ correction.

These results demonstrate that the JV curves of normal CdTe solar cells can be completely described by the equation

$$J(V') = [J_0 \exp(qV'/AkT) - [J_{LO} \times \eta_c(V')]] \qquad (4)$$

where 6 parameters – J_o, R_s, A, J_{LO}, X_C , and V_{FB} – can uniquely specify the entire light JV curve. We have shown how they can be obtained using measurements at 2 or more light intensities. There is no need to invoke weak diodes, nonuniformity, double junctions or photoconductivity. The only exception to this is when blocking contacts occur which primarily influence the current beyond V_{oc}. Interpretation of the physical origins of the 6 parameters above, especially J_o and X_c will require additional insight into the electronic mechanisms.

Table VIII. Standard JV parameters V_{oc}, J_{sc}, and FF; R_{oc} and G_{sc} from the slopes at OC or SC; junction parameters A and J_o and series resistance R from analysis of the 1% light curve; and fitting parameter X_c, all for three devices having wide range of FF.

Piece	V_{oc} (V)	J_{sc} (mA/cm^2)	FF (%)	Eff (%)	R_{oc} (Ω-cm^2)	G_{sc} (S/cm^2)	A	J_o (mA/cm^2)	R (Ω-cm^2)	X_c
VT174.1	0.80	21.2	72.1	12.2	4.7	0.5	1.4	2E-8	2.8	25
VT176.4	0.80	23.9	62.0	12.0	6.4	2.0	1.4	1E-8	5.3	13
VT176.1	0.77	20.9	56.5	8.9	6.9	3.5	1.5	3E-8	4.3	4.5

Collaboration

CdS films on Ga_2O_3-coated TEC15 and Ga_2O_3/ITO-coated flexible Pilkington glass substrates were sent to the University of Toledo for stress-piezoelectric analysis and device fabrication. Completed VT cells fabricated with and without $CdCl_2$ treatment and Cu contacts were supplied to Colorado School of Mines (CSM) for admittance spectroscopy analysis in an effort to correlate these processing variables with the spectral signatures indicative of defect levels. Brian McCandless attended the National CdTe R&D Team meeting on March 9-10, 2006. Brian co-led the Materials Chemistry sub-team with Tim Ohno (CSM) and made presentations in sessions for the Device Physics and Materials Chemistry teams and at a workshop focused on CdTe solar cell open circuit voltage.

References

[1] W. Shafarman, R Klenk, B McCandless "Device and material characterization of $Cu(InGa)Se_2$ solar cells with increasing bandgap," J. Appl. Phys. **79**, 7324 (1996).
[2] S. Hegedus, "Current voltage analysis of a-Si solar cells including voltage dependent collection," Prog in Photovoltaics **5**, 151 (1997).

Best regards,

Robert W. Birkmire
Director

RWB/eak

Cc: Brian McCandless, IEC
Kevin Dobson, IEC
Steven Hegedus, IEC
Paula Newton, IEC
Gerri Hobbs, OVPR UD
Carolyn Lopez, NREL